Salt-Triggered Peptide Folding and Consequent Self-Assembly into Hydrogels with Tunable Modulus

Bulent Ozbas,[†] Juliana Kretsinger,[‡] Karthikan Rajagopal,[‡] Joel P. Schneider,[*,‡] and Darrin J. Pochan[*,†]

Materials Science and Engineering Department, Delaware Biotechnology Institute, Chemistry and Biochemistry Department, University of Delaware, Newark, Delaware 19716

Received April 27, 2004

ABSTRACT: Intramolecular folding events, triggered by the presence of salt, induce the self-assembly of β-hairpin peptides into hydrogel networks at physiological conditions. At pH 7.4 and low ionic strength solution conditions, dilute, homogeneous solutions of peptide ($\leq$2 wt %) exhibit the viscosity of pure water. Circular dichroism spectroscopy shows that, at pH 7.4 in the absence of salt, peptides are unfolded. By raising the ionic strength of the solution, electrostatic interactions between charged amino acids within the peptide are screened, and a β-hairpin conformation is adopted. Folded β-hairpin molecules supramolecularly assemble via hydrophobic collapse and hydrogen bonding into a three-dimensional hydrogel network. FTIR and X-ray scattering data demonstrate that these hydrogels are rich in β-sheet. Dynamic oscillatory rheological measurements demonstrate that the resultant supramolecular structure forms an elastic material whose structure, and thus modulus, can be tuned by salt concentration and temperature. Storage moduli of hydrogels increase with increasing salt concentration. Robust hydrogelation is also observed in cell growth media at physiological conditions. Transmission electron microscopy reveals that the hydrogel elasticity arises from a network nanostructure consisting of semiflexible fibrillar assemblies.

Introduction

Hydrogels are collectively an important class of biomaterial that have extensive uses in tissue engineering and drug delivery applications.[1,2] Self-assembly strategies provide precise control in order to construct new hydrogel materials with desired nano- and microstructures that can be responsive to environmental conditions, such as temperature,[3,4] pH,[5] electric field,[6] ionic strength,[7,8] or light.[9,10] In our initial work we introduced pH[11] and temperature[12] triggered hydrogelation of β-hairpin peptides. These molecules exhibited a pH- and temperature-dependent intramolecular folding event that resulted in a reversible intermolecular self-assembly process leading to hydrogel scaffold formation. In general, by controlling the peptide folding event, it is possible to design responsive materials that undergo self-assembly with desired stimuli. In addition, the self-assembly process can be controlled in order to engineer desired morphological and mechanical properties. In this paper we introduce salt concentration as a trigger to induce the β-hairpin intramolecular folding event followed by self-assembly into a supramolecular elastic network. The rate of self-assembly, and thus final gel rheological properties, are tuned by ionic strength of the peptide solutions. Importantly, the formation of these physical hydrogels does not involve any chemical cross-linking and can be performed at physiological temperature and pH.

There are different strategies reported in the literature to make polymeric gels that are responsive to stimuli, e.g., undergo sol−gel or swelling transitions as a response to changes in physical or chemical environmental conditions. While temperature and pH are the most prevalent stimuli, ionic strength is also used to trigger gelation by phase transition, self-assembly, or polymer conformational changes. The formation of salt complexes can change solution and self-assembly properties of block copolymers that form self-assembled structures like spherical or wormlike micelles. For example, the type and amount of salt have been shown to change aggregation properties and, thus, the elasticity of the networks formed by Pluronic-based block copolymer systems.[13−15] Chemical hydrogels of synthetic polymers such as *N*-isopropylacrylamide, well-known to exhibit thermal responsiveness due to an LCST-type phase transition,[16,17] also exhibit salt-induced volume phase transitions.[7] At relatively high salt concentrations (or at temperatures higher than the LCST), hydrophobic interactions dominate and lead to the precipitation of the chemically cross-linked polymer chains, causing gel collapse. Swelling of hydrophilic networks such as poly(acrylic acid) and poly(methacrylic acid) hydrogels caused by ionic strength[18,19] and pH[20,21] has been explored for the potential to produce responsive biomaterials.

Gelation behavior of biomacromolecules, such as gelatin,[22] polysaccharides,[3] and β-lactoglobulin,[23] is extensively studied in the literature. It is well-known that by applying thermal treatments, these macromolecules undergo secondary structure (conformational) transitions, resulting in the formation of intermolecular network structures. For example, gelatin forms hydrogels with decreasing temperature via the formation of triple-helical physical junctions.[24] Rheological studies on gelatin gels revealed that the viscoelastic properties are highly dependent on processing conditions, such as rate of cooling, degree of undercooling, and concentration.[22] However, because of the polyelectrolytic nature of biomacromolecule solutions, the ionic strength is also a vital parameter to control assembly properties. Effects of ionic strength on biomacromoleculer gel networks, such as pectin,[25] β-lactoglobulin,[26,27] welan,[28] and gela-

[†] Materials Science and Engineering Department, Delaware Biotechnology Institute.
[‡] Department of Chemistry and Biochemistry.
* Author of correspondence: e-mail pochan@udel.edu., schneijp@udel.edu.

10.1021/ma0491762 CCC: $27.50
Published on Web 08/25/2004

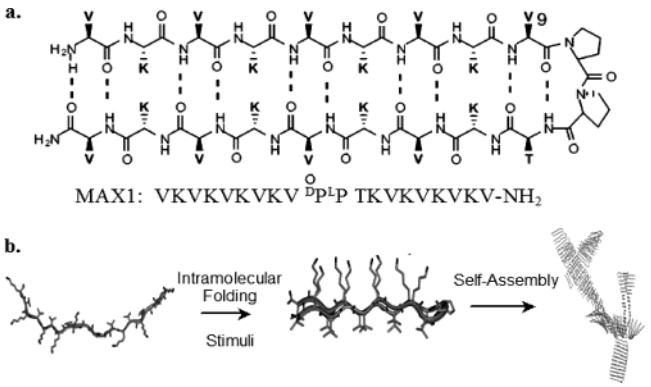

Figure 1. (a) 20 residue long sequence and proposed β-hairpin structure of Max1. (b) Unordered state structure and proposed self-assembly pathway of Max1. Intramolecular folding event is triggered via application of a stimuli and Max1 folds and self-assembles into β-sheet rich fibrillar supramolecular structures.

tin,[29] have been well studied due to their importance in food processing and pharmaceutical applications. In general, increasing the ionic strength of these solutions results in an increase in network elasticity due to the formation of intermolecular salt-bridge physical cross-links.

There is a great interest in mimicking the stimuli responsive self-assembly routes of biomacromolecules with well-defined sequences of oligo- and polypeptides because of their potential applications as responsive biomaterials. Self-assembly of oligopeptides into β-sheet-rich, β-amyloid-like structures triggered by ionic strength and pH has been investigated as a biomimetic material formation strategy.[30−34] For example, Caplan et al. showed that self-assembly and resultant gel properties of an oligopeptide, with an alternating sequence of hydrophobic amino acid residues with positively or negatively charged amino acids, can be altered by the ionic strength of the solution.[32] In addition, elastin−mimetic peptides,[35] hybrid molecules with coiled-coil protein−synthetic polymer domains,[36] and leucine zipper polypeptide domains with an additional polyelectrolyte segment[37] form responsive hydrogels that undergo gelation with temperature or pH at appropriate ionic strength.

Here we present salt-triggered physical hydrogel formation via intramolecular folding and consequent intermolecular self-assembly of a 20 amino acid β-hairpin molecule (Max1) at low peptide concentrations (2 wt %) under physiological conditions. The molecule, shown in Figure 1a, consists of two strands composed of an alternating sequence of valine (V), (isopropyl hydrocarbon side chain) and lysine (K) (primary amine capped side chain) amino acid residues that are connected with a tetrapeptide turn sequence (-V^{D}PPT-) that adopts what is known as a type II′ turn.[38,39] While V is a nonpolar residue, K is positively charged and hydrophilic at pH values around physiological conditions (~7.4). Electrostatic forces and hydrophobic interactions, due to the charges on K residues and nonpolar V residues, respectively, are the primary intramolecular parameters that can be used to control the folding of the molecule. In the folded state the molecule is facially amphiphilic, having all V residues on one face of the hairpin with K residues on the other (Figure 1b). Once the molecule is folded, self-assembly is driven by both lateral intramolecular hydrogen bonding and facial hydrophobic interactions.[11,12] Therefore, these molecules are specifically designed to first fold and then self-assemble into quaternary structures rich in β-sheet that give rise to gel properties of the system. Final elastic properties of the self-assembled structure can be tuned by salt concentration. In addition, because of the facial hydrophobic association, temperature can also be used as a parameter in controlling gelation kinetics. Therefore, these molecules are designed to exhibit sol−gel transitions when solution conditions (ionic strength, temperature, pH) are adjusted to physiological levels, providing significant potential uses for tissue engineering applications.

Experimental Section

Sample Preparation. Max1 was prepared on amide resin via automated Fmoc-based solid-phase peptide synthesis employing an ABI 433A peptide synthesizer and HBTU/HOBT activation. The details of peptide preparation are given elsewhere.[11] Hydrogels were prepared by dissolving the lyophilized peptide first in DI water and the desired final solution conditions were achieved by the subsequent addition of buffer and salt containing solution. Bis-trispropane was used for buffering the solution at pH 7.4 with the exception of the X-ray study in which TRIS buffer was used.

Circular Dichroism. CD spectra were collected using an Aviv model 215 spectropolarimeter. Measurements were done at either 20 or 37 °C. Wavelength scans, between 190 and 260 nm, for 2 wt % Max1 (pH 7.4, 50 mM BTP) with 0 and 150 mM KF solutions were obtained in a 0.01 mm detachable quartz cell. The wavelength spectra were taken after 2 h of dissolution of peptide in DI water and buffer solution. For time-dependent studies, the mean residue ellipticity, $[\theta]$, was measured at 218 nm. $[\theta]$ was calculated from the equation $[\theta] = (\theta_{obs}/l01c)/r$, where θ_{obs} is the measured ellipticity in millidegrees, l is the length of the cell (centimeters), c is the concentration (molar), and r is the number of residues.

Infrared Spectroscopy. IR spectra were taken on a Nicolet Magna-IR 860 spectrometer. Deuterated Max1*nDCl was prepared by lyophilizing the TFA salt of peptide once from 0.1 M HCl and twice from D_2O. Samples were kept in a temperature-controlled water bath at 20 °C for 2 h before measurements were immediately taken at room temperature in a zinc selenide flow cell with 30 μm path length. The equipment was operated at 1 cm^{-1} resolution, and the spectrum recorded was an average of 100 scans.

Wide-Angle X-ray Scattering. X-ray spectra of the hydrated gels were collected at the National Synchrotron Light Source, Brookhaven National Laboratory, beamline, X10A. Hydrogel was smeared on Kapton tape just before taking measurements in order to avoid dehydration. Data were collected for 10 min on a two-dimensional Bruker CCD array. Peptide solutions were buffered with 125 mM TRIS. Measurements were done at room temperature.

Rheology. Dynamic time and frequency sweep experiments were performed in a strain-controlled Rheometrics ARES rheometer with 25.0 mm diameter parallel plate geometry and 0.5 mm gap distance. Lyophilized peptide was dissolved in deionized water and buffer or cell growth media solution at 10 °C in order to suppress folding and gelation before the sample is loaded into the rheometer. After the sample was loaded, temperature was increased to either 20 or 37 °C. Standard low-viscosity mineral oil was used to insulate the sides of the plate in order to suppress evaporation. Control experiments showed that mineral oil had no effect on rheological measurements. Strain sweep experiments were performed to determine the linear viscoelastic regime in which all rheological experiments were performed. Dynamic time sweep experiments were performed with a frequency and strain of 6 rad/s and 1%, respectively. Frequency sweep experiments were performed with a frequency and strain of 0.1−100 rad/s and 5%, respectively.

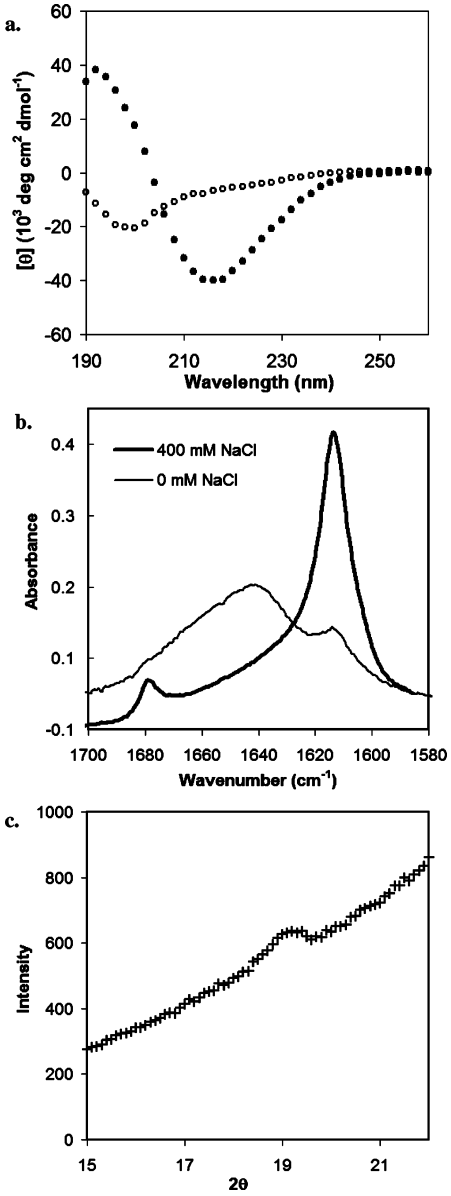

Figure 2. (a) CD spectra of 2 wt % Max1, pH 7.4 solution with 0 mM (○) and 150 mM (●) KF at 20 °C. (b) FTIR spectrum of 2 wt % Max1 solution, pH 7.4 with 0 and 400 mM NaCl. (c) WAXS spectrum of 3 wt % Max1 solution, pH 7 with 150 mM NaCl.

Transmission Electron Microscopy. A very thin layer of hydrogel was applied to carbon-coated copper grids. The samples were negatively stained by placing a drop of 2% (w/v) uranyl acetate aqueous solution on the grid. The excess of the solution was blotted with filter paper, and the sample was subsequently left to dry. To prevent the formation of salt and/or buffer crystals and to image the individual fibrils clearly, hydrogel with 2 wt % peptide concentration was diluted to ~0.1 wt % in DI water. To disperse the fibrils evenly in the solution, gentle sonication was employed with a tip sonicator. Bright field images of hydrogel nanostructure were taken on a JEOL 2000-FX transmission electron microscope at 200 kV accelerating voltage on both a Gatan CCD camera and Kodak negative films.

Results and Discussion

***β*-Sheet Structure.** Figure 2 shows CD spectra of 2 wt % Max1 solutions at pH 7.4 and 20 °C for different salt concentrations. Both spectra shown were taken after 2 h of dissolution of Max1 with DI water and buffer solution. The minima at 218 nm for the peptide solution with 150 mM KF indicates that at 2 wt % gelation concentrations Max1-folds and adopts secondary structure rich in β-sheet. However, 2 wt % Max1 at identical pH in the absence of salt did not show significant regular secondary structure even after 2 h, indicating the peptide remains unfolded without the presence of added salt.

Folding of the peptide molecule to β-hairpin structure and subsequent β-sheet formation with the presence of salt were also confirmed by FTIR spectroscopy. The FTIR spectrum of Max1 solution at pH 7.4 and with 400 mM NaCl, between 1580 and 1700 cm^{-1}, is given in Figure 2b. The amide I band for unordered peptide in D_2O is centered around 1645 cm^{-1}.[40] The shift of the amide I band from 1644 to 1614 cm^{-1} suggests that the peptide adopts β-sheet conformation in 400 mM NaCl solution.[41] The weak band in the spectrum at 1680 cm^{-1} may be an indication of antiparallel β-sheet structure.[11] For Max1 solution without NaCl, a very broad spectrum is obtained in the plotted range. The strong band at 1644 cm^{-1} suggests that peptide is in an unordered state. However, the weak band at 1614 cm^{-1} also indicates the presence of a small amount of folded β-hairpin molecules in the solution. We believe that folding of some of Max1 is due to both the excess buffer salt and a relatively high concentration of peptide in the solution. It was shown that peptide concentration has an effect on the kinetics of β-sheet formation.[11] Therefore, this small amount of β-sheet amide I signal in the context of the high concentration of peptide and lack of gelation (vide infra) is insignificant.

Since Max1 has a net positive charge at pH 7.4 due to the primary amines on the lysine residues, the data suggest that it cannot fold due to the electrostatic repulsion between the strands. Therefore, when the positive charges on the lysine residues are screened by Cl^- ions, the intramolecular folding event is favored, leading to formation of β-hairpin structure. Increased salt concentrations may also drive the hydrophobic association of residues, which should also contribute to folding and self-assembly. Both CD and FTIR data show that the folding mechanism is triggered by ionic strength of the solution. In our previous papers it was shown that folding can be triggered by pH[11] and temperature.[12] Similar to the effect of salt, when pH is used as a stimulus, lysine residues are deprotonated at high pH and Max1 folds. When folded, Max1 is capable of self-assembly into higher order structures by intermolecular hydrogen bonding and hydrophobic interactions. The kinetics of β-sheet formation, structure of assembled aggregates, and the consequent hydrogel network properties will be discussed.

Crystallographic β-sheet structure is observed in the final hydrogels using X-ray scattering techniques. Figure 2c shows the wide-angle curves for a hydrogel consisting of 3 wt % of Max1 and 150 mM NaCl. The scattering peak corresponds to 4.7 Å. This is the characteristic signature of the interchain distance in β-sheet-rich structures.[30] Since the measurements were taken without drying out the hydrogels, the scattering background contribution at high angles due to the water structure is significant.

Rheological Properties of Hydrogels. Hydrogels formed via the intramolecular folding mechanism exhibit rigid viscoelastic properties, even at low concentration of Max1 peptide, as observed by dynamic oscillatory techniques. Figure 3a shows frequency sweep measure-

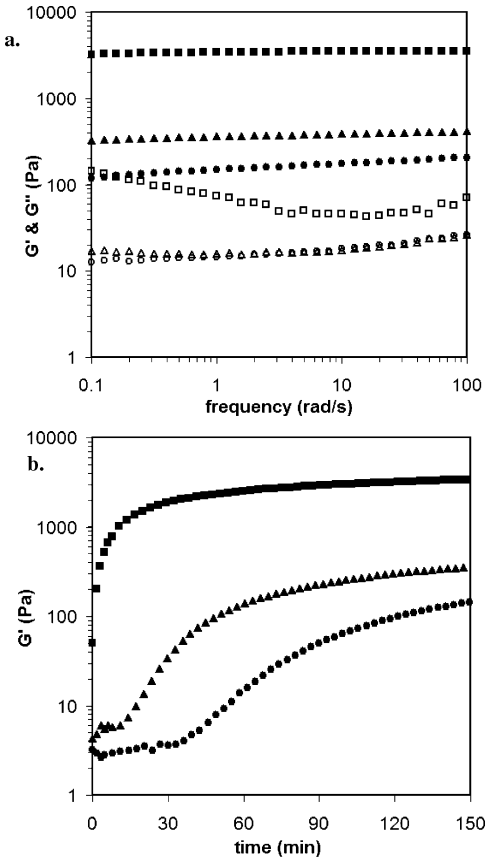

Figure 3. (a) Dynamic frequency sweep (5% strain) of 2 wt % Max1, pH 7.4 solution with 20 mM (G', ●; G'', ○), 150 mM (G', ▲; G'', △), and 400 mM (G', ■; G'', □) NaCl at 20 °C. (b) Dynamic time sweep (1% strain, 6 rad/s) of 2 wt % Max1 solution with 20 mM (G', ●), 150 mM (G', ▲), and 400 mM (G', ■) NaCl at 20 °C.

ments from 10^{-1} to 10^{2} rad/s for 2 wt % Max1 peptide solutions at 20, 150, and 400 mM NaCl concentrations. Before the frequency sweep measurements peptide solutions were allowed to gel for 2.5 h in the rheometer (Figure 3b). For Max1 solution with 400 mM NaCl the equilibrium storage modulus (G') is ∼3000 Pa. Decreasing salt concentration resulted in the decrease of both G' and loss modulus (G'') values. A hydrogel with low rigidity (G' ∼100 Pa) is formed when only 20 mM NaCl is present in the solution. Max1 at pH 7.4 without added NaCl did not exhibit any gelation even after 3 h with G' values approximately 1 Pa. (The response of the sample to the applied strain was negligible; torque values were under the detection limit of the instrument leading to insignificant measurements that are not shown.) For all three samples with salt, G' values are at least 1 order of magnitude greater than the G'' values. Also, for all NaCl concentrations, the G' values are essentially independent of the frequency in the studied range, exhibiting no crossover point between G' and G'' at low frequencies. These characteristics are a clear signature of cross-linked networks. The frequency sweep data in Figure 3a suggest that these solutions form rigid, solidlike hydrogels with properties similar to covalently cross-linked polymer gels.[42]

The spectroscopy data in Figure 2 suggest that in solutions without salt the electrostatic repulsion of lysine residues keeps the peptide unfolded, thus preventing self-assembly into a network structure. However, once the molecule is folded, self-assembly can occur. Since all valine residues are positioned on one side of the molecule in the folded state (Figure 1b), facial hydrophobic dimerization can occur. Additional intermolecular hydrophobic interactions and hydrogen bonding can consequently occur, forming an interconnected network. Importantly, the differences in the hydrogel rigidity with different salt concentrations, as shown in Figure 3a, reveal that not only can the self-assembly be triggered with ionic strength but also that the resultant nanostructure can be predictably altered by the ionic strength of the medium. Figure 3b shows the increase in G' values during self-assembly of Max1 solution for the same peptide concentration of 2 wt %. This experiment clearly demonstrates the differences in the kinetics of self-assembly and network formation for different salt concentrations. Max1 solution with 400 mM NaCl shows a rapid increase in its G' value in the first couple of minutes of the self-assembly process while the 20 and 150 mM NaCl solutions stiffened with a relatively slow rate. In fact, the 20 mM NaCl solution G' values do not change significantly for 3000 s, remaining around 2−3 Pa. This lag time is shorter for 150 mM (∼1000 s) and does not exist for 400 mM salt solution. Figure 3b clearly suggests that faster kinetics of self-assembly and self-assembly due to higher ionic strength results in stiffer gels. The order of magnitude differences in stiffness between solutions with the same peptide concentration presumably arise from more highly cross-linked networks due to faster assembly kinetics; this possibility is currently being investigated.

Nanostructure. The nanostructure of the hydrogels that results in elastic properties was studied by transmission electron microscopy (TEM). Figure 4a shows the TEM image of a 2 wt % Max1 hydrogel network formed at pH 7.4 with 400 mM NaCl. The micrograph reveals the highly interconnected fibrillar network structure at the nanoscale. Although it cannot be directly seen from the TEM micrograph, we believe that most of the junction points formed during self-assembly are intersecting fibrils and are not simply entanglements of long, nonintersecting fibrils (although certainly entanglements contribute to the modulus). These cross-link points between the fibrils, although not covalent in origin, are permanent and are formed via both hydrogen-bonding and hydrophobic interactions. Frequency sweep data, given in Figure 3a, also support this hypothesis; G' is insensitive to frequency and is an order of magnitude greater than G'', and no G'' to G' crossover exists. Because of the evaporation of the water prior to imaging and relatively high salt concentration, the 2 wt % structure is very dense with some parts of the network embedded in precipitated salt. Therefore, the hydrogel was diluted with DI water by approximately a factor of 20 (to ∼0.1 wt % peptide), and a sample was immediately prepared for TEM imaging. Figure 4b shows the more dilute fibrillar assemblies. Contour lengths of the fibrils are on the order of micrometers. Although drying during sample preparation may cause conformational changes along the fibril axis, micrographs suggest that the self-assembled fibrils are semiflexible. Importantly, the widths of the fibrils are monodisperse in size and approximately 3 nm. The proposed local self-assembled structure and the dimensions are shown in Figure 5. Insight II modeling shows that the strand axis of the folded peptide is 32 Å in length, and the distance from valine face to lysine face is ∼10 Å. The ∼3 nm width of the fibrils is in very good

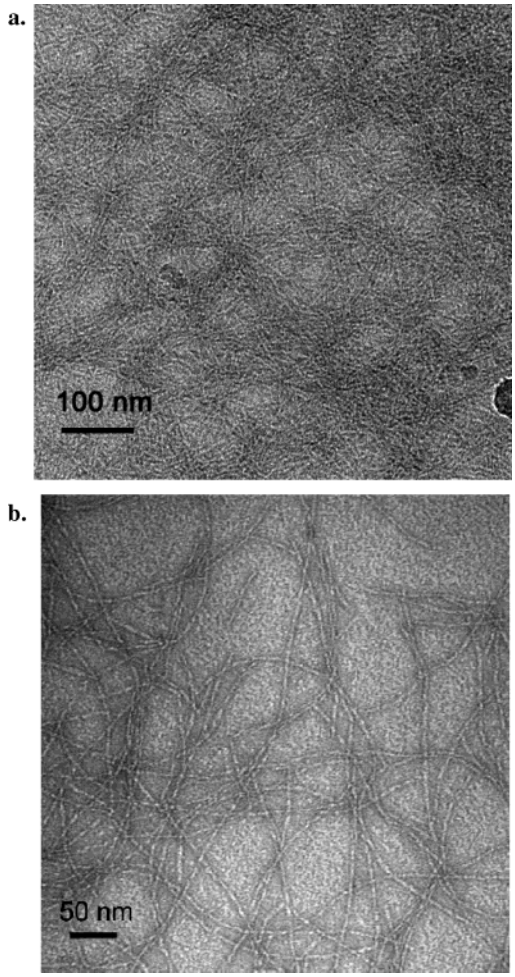

Figure 4. Negatively stained (uranyl acetate) TEM images of self-assembled structure of hydrogels. (a) Densely interconnected network of 2 wt % Max1, pH 7.4, 400 mM NaCl solution. (b) Fibrillar assemblies of a diluted hydrogel (final concentration after dilution: ~0.1 wt %).

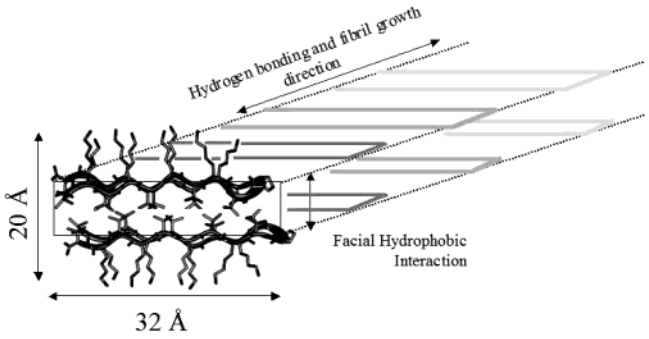

Figure 5. Proposed structure of self-assembled Max1 β-hairpin molecules in a fibril. The stand axis of the molecule is 32 Å, and the cross-section thickness is 20 Å. The long axis of the structure shows the hydrogen bonding and fibril growth direction.

agreement with these molecular dimensions. TEM data along with the CD data strongly suggest that Max1 is in the folded state during the self-assembly process. In the proposed structure in Figure 5 β-turns are shown to be on the same side of the fibrillar bilayer for simplicity. To fully understand the self-assembled structure, e.g., parallel or antiparallel β-sheet formation between hairpin molecules, and thickness of the fibrils, direct characterization of cross-links, more X-ray scattering, and microscopy studies are underway.

Effect of Temperature on Folding and Gelation. CD and rheology results clearly demonstrate that folding and subsequent gelation of β-hairpin molecules can be triggered with a change in salt concentration at pH 7.4. This type of response provides an opportunity for using these materials at physiological conditions. Therefore, the self-assembly and gelation behavior of these molecules was studied at physiological temperature, 37 °C. In a previous paper,[12] it was shown that folding and β-sheet formation of Max1 are temperature-dependent. CD studies indicated that for Max1 the transition temperature from an unordered, random coil state to folded β-sheet structure is around 25 °C at pH 9 and low (20 mM) salt. This transition was shown to be tunable to higher temperatures via changing the hydrophobic character of the assembling peptide.

To observe the effect of temperature on the self-assembly triggered by ionic strength, gelation was monitored over 2.5 h by dynamic time sweep experiments at 20 and 37 °C. In Figure 6a, the change in G' is plotted as a function of time for 2 wt % Max1 at pH 7.4 and 150 mM NaCl solution. In both cases Max1 solutions were initially kept at 10 °C to suppress folding before measurements were taken. An instantaneous increase in G' at 37 °C indicates that the peptide formed a network structure immediately during self-assembly. Contrastingly, at 20 °C the increase in elastic response of the hydrogel is slower, showing an insignificant increase in G' for the first 15 min of self-assembly. This behavior can be beneficial for potential applications in which one desires a solution with viscouslike behavior at room temperature while exhibiting a fast gelation response when exposed (e.g., injected in vivo) to body temperature and salt concentration. Figure 6a clearly shows that at physiologically relevant conditions (e.g., pH 7.4, 37 °C) gelation leading to a material that displays useful rigidity occurs in about 10 min. The frequency sweep measurement (Figure 6b) taken at the end of 2.5 h gelation period at 37 °C indicates that a rigid hydrogel ($G' > G''$) was formed with a G' value around 2000 Pa. During gelation at both temperatures G'' values (not shown) were constant and always well below (>1 order of magnitude) the G' values throughout the gelation process. In all samples, even during the early stages of gelation, $G' > G''$. Similar behavior has also been seen in the gelation of biomacromolecules.[43] Similar to ionic strength effect, the formation of stiffer gels assembled at higher temperatures may be due to structural differences at the nanoscale. A faster rate of folding and consequent self-assembly can form network structure more dense in number of junction points, leading to higher G' values. Although the exact nanostructural premise for the observed difference in G' is not fully known at this time, these data show that the rigidity of Max1 hydrogel can be easily and predictably controlled by either temperature or salt concentration.

The rate of β-sheet formation of Max1 peptide was studied by CD. Figure 6c shows the rate of change of ellipticity, measured at 218 nm, at 20 and 37 °C for 2.0 wt % Max1, pH 7.4, with 150 mM KF solution. KF is used as the electrolyte since it is optically silent and conducive to CD measurements. CD data reveal that in the early stages of self-assembly β-sheet formation is very fast at 37 °C. The rate of β-sheet formation during the first 5 min is significantly high, reaching a plateau region after 15 min. However, at 20 °C the rate of β-sheet formation is slower. The differences in the

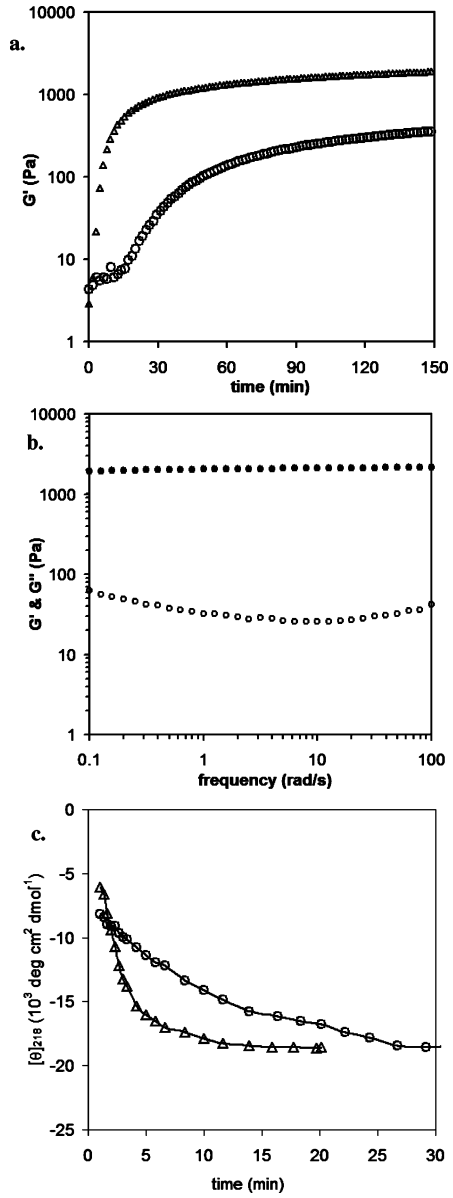

Figure 6. (a) Dynamic time sweep (1% strain, 6 rad/s) of 2 wt % Max1, pH 7.4 solution with 150 mM NaCl at 20 °C (G', ○) and 37 °C (G', △). (b) Frequency sweep (5% strain) of hydrogel at 37 °C after 2.5 h of gelation (G', ●; G'', ○). (c) Time-dependent mean molar ellipticity at 218 nm ($[\theta]_{218}$) of 2.0 wt % Max1, pH 7.4 with 150 mM NaCl at 20 °C (○) and 37 °C (△).

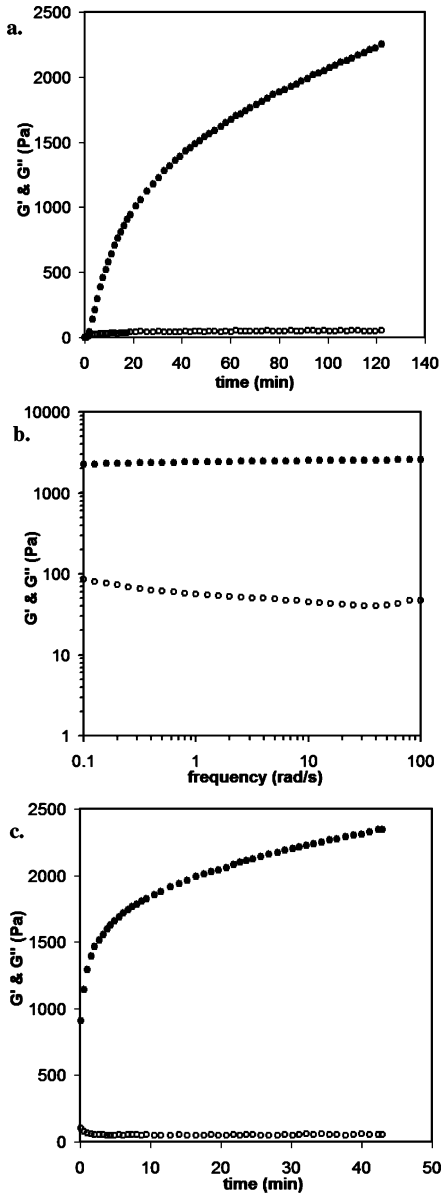

Figure 7. Rheology data (G', ●; G'', ○) of 2 wt % Max1 solution in cell growth media at 37 °C. (a) Gel formation (1% strain, 6 rad/s frequency), (b) frequency sweep (5% strain), and (c) G' and G'' recovery of hydrogel (1% strain, 6 rad/s frequency) after cessation of high amplitude of strain (1000%, 6 rad/s).

kinetics of β-sheet formation and, thus, self-assembly are in accordance with the rheological measurements shown in Figure 6a. At 37 °C, changes in G' and θ_{218} values are very rapid at the early stages of self-assembly, while at 20 °C the rates of change of both values are much slower. Therefore, higher storage moduli for gels formed at 37 °C may be attributed to the fast rate of β-sheet formation and consequent fast rate of self-assembly. At the initial stages of self-assembly, the high rate of self-assembly results in more nucleation sites for β-sheet-rich fibril growth, and consequently, a network is formed with more junction points. This working mechanism is consistent with all of the data obtained thus far.

Gelation in Cell Growth Media. For biomaterials applications it is important to understand the response of Max1 to biologically relevant conditions. Therefore, the gelation of Max1 was studied in serum-free DMEM cell growth media. Figure 7a shows G' and G'' during the gelation of Max1 in cell growth media at 37 °C (mammalian cell culturing conditions). At the end of 2 h of gelation G' and G'' values were 2300 and 50 Pa, respectively. It can be seen that the rate of increase in G' value at the end of 2 h is still significant. To eliminate the effects of evaporation that would result in an increase in peptide concentration and G' value, the dynamic time sweep experiment was stopped after 2 h of gelation. (This continuing increase in the G' value without showing a final value has also been seen in gelatin gels.[44]) Frequency sweep data, shown in Figure 7b, indicate that the Max1−cell growth media solution forms a rigid gel with G' values ∼2500 Pa. The properties of the frequency sweep data of the media induced hydrogel ($G' > 10G''$, G' independent of frequency) are similar to those shown in Figure 2a. The response of the hydrogel to significant shear was studied by monitoring recovery of G' after application of high magnitude

of strain (1000% at 6 rad/s) to the gelled solution. Since the applied strain is well outside the linear regime, G' and G'' values are not shown. Figure 7c shows that, after cessation of shear and the immediate application of 5% strain at 6 rad/s, G' instantaneously recovers almost 50% of its initial value. When recovery data are compared with the gelation data (Figure 7a), it can be seen that the rate of increase of G' is faster than the rate during initial gelation. This suggests that during the application of high magnitude of strain the physically cross-linked, self-assembled network structure is fractured, resulting in the decrease of connectivity and, thus, elasticity of the material. After the cessation of shear, the network can quickly reheal as manifested in the immediate recovery of significant network stiffness. This experiment demonstrates that these hydrogels are processable and can recover initial rheological properties after being disturbed by external mechanical forces. This ease of processability and recovery can be advantageous for tissue engineering applications (e.g., in vivo injection).

Conclusions

Rigid hydrogels are formed via folding and self-assembly of β-hairpin peptides. While Max1 is in a random coil conformation at physiological pH (7.4), the addition of salt to the solution results in the formation of self-assembled structures rich in β-sheet. Rheological data demonstrate that peptide solutions form gels with G' at least 1 order of magnitude greater than G''. In addition, G' is insensitive to frequency, indicating that the network is similar in elastic properties to chemically cross-linked polymer gels. Kinetics of self-assembly as well as storage modulus of the hydrogels can be tuned by the ionic strength of the peptide solution. The network structure is composed of dense fibrillar assemblies that are cross-linked to each other by physical junction points possibly due to facial hydrophobic interactions and hydrogen bonding. The width of the fibrils is approximately 3 nm, and this dimension is in a good agreement with the folded state of the hairpins in the self-assembled state. Salt-triggered self-assembly and consequent gelation properties are also tuned by temperature. At 37 °C, the kinetics of β-sheet formation and gelation are faster than at 20 °C, resulting in stiffer gels. In addition, Max1 forms rigid and processable hydrogels in cell growth media at physiological conditions. Thus, properly designed peptides can be triggered by salt to intramolecularly fold and consequently intermolecularly assemble into supramolecular structures that result in hydrogels with tunable modulus.

Acknowledgment. This work was supported by National Institutes of Health (P20-RR17716) and National Science Foundation (0348323). We thank the National Synchrotron Light Source, Brookhaven, for the beam time and the W. M. Keck foundation for funding the College of Engineering Electron Microscopy Lab. We thank Professor Norman Wagner for thoughtful discussions.

References and Notes

(1) Lee, K. Y.; Mooney, D. J. *Chem. Rev.* **2001**, *101*, 1869−1879.
(2) Peppas, N. A.; Bures, P.; Leobandung, W.; Ichikawa, H. *Eur. J. Pharmacol. Biopharm.* **2000**, *50*, 27−46.
(3) Nijenhuis, K. T. In *Thermoreversible Networks*; Springer-Verlag Berlin: 1997; Vol. 130, pp 1−12.
(4) Jeong, B.; Bae, Y. H.; Lee, D. S.; Kim, S. W. *Nature (London)* **1997**, *388*, 860−862.
(5) Torres-Lugo, M.; Peppas, N. A. *Macromolecules* **1999**, *32*, 6646−6651.
(6) Tanaka, T.; Nishio, I.; Sun, S. T.; Uenonishio, S. *Science* **1982**, *218*, 467−469.
(7) Annaka, M.; Motokawa, K.; Sasaki, S.; Nakahira, T.; Kawasaki, H.; Maeda, H.; Amo, Y.; Tominaga, Y. *J. Chem. Phys.* **2000**, *113*, 5980−5985.
(8) Zhao, B.; Moore, J. S. *Langmuir* **2001**, *17*, 4758−4763.
(9) Collier, J. H.; Hu, B. H.; Ruberti, J. W.; Zhang, J.; Shum, P.; Thompson, D. H.; Messersmith, P. B. *J. Am. Chem. Soc.* **2001**, *123*, 9463−9464.
(10) Lee, J.; Macosko, C. W.; Urry, D. W. *Macromolecules* **2001**, *34*, 4114−4123.
(11) Schneider, J. P.; Pochan, D. J.; Ozbas, B.; Rajagopal, K.; Pakstis, L.; Kretsinger, J. *J. Am. Chem. Soc.* **2002**, *124*, 15030−15037.
(12) Pochan, D. J.; Schneider, J. P.; Kretsinger, J.; Ozbas, B.; Rajagopal, K.; Haines, L. *J. Am. Chem. Soc.* **2003**, *125*, 11802−11803.
(13) Bromberg, L. *J. Phys. Chem. B* **1998**, *102*, 10736−10744.
(14) Liu, L. Z.; Wan, Q.; Liu, T. B.; Hsiao, B. S.; Chu, B. *Langmuir* **2002**, *18*, 10402−10406.
(15) Pandit, N.; Trygstad, T.; Croy, S.; Bohorquez, M.; Koch, C. *J. Colloid Interface Sci.* **2000**, *222*, 213−220.
(16) Hirokawa, Y.; Tanaka, T. *J. Chem. Phys.* **1984**, *81*, 6379−6380.
(17) Otake, K.; Inomata, H.; Konno, M.; Saito, S. *Macromolecules* **1990**, *23*, 283−289.
(18) Horkay, F.; Basser, P. J.; Hecht, A. M.; Geissler, E. *Macromolecules* **2000**, *33*, 8329−8333.
(19) Horkay, F.; Tasaki, I.; Basser, P. J. *Biomacromolecules* **2000**, *1*, 84−90.
(20) Eichenbaum, G. M.; Kiser, P. F.; Simon, S. A.; Needham, D. *Macromolecules* **1998**, *31*, 5084−5093.
(21) Philippova, O. E.; Hourdet, D.; Audebert, R.; Khokhlov, A. R. *Macromolecules* **1997**, *30*, 8278−8285.
(22) Nijenhuis, K. T. *Colloid Polym. Sci.* **1981**, *259*, 1017−1026.
(23) Tobitani, A.; RossMurphy, S. B. *Macromolecules* **1997**, *30*, 4855−4862.
(24) Guo, L.; Colby, R. H.; Lusignan, C. P.; Whitesides, T. H. *Macromolecules* **2003**, *36*, 9999−10008.
(25) Yoo, S. H.; Fishman, M. L.; Savary, B. J.; Hotchkiss, A. T. *J. Agric. Food Chem.* **2003**, *51*, 7410−7417.
(26) Ikeda, S.; Foegeding, E. A.; Hagiwara, T. *Langmuir* **1999**, *15*, 8584−8589.
(27) Jeyarajah, S.; Allen, J. C. *J. Agric. Food Chem.* **1994**, *42*, 80−85.
(28) Hember, M. W. N.; Morris, E. R. *Carbohydr. Polym.* **1995**, *27*, 23−36.
(29) Hone, J. H. E.; Howe, A. M.; Cosgrove, T. *Macromolecules* **2000**, *33*, 1199−1205.
(30) Lashuel, H. A.; LaBrenz, S. R.; Woo, L.; Serpell, L. C.; Kelly, J. W. *J. Am. Chem. Soc.* **2000**, *122*, 5262−5277.
(31) Aggeli, A.; Bell, M.; Carrick, L. M.; Fishwick, C. W. G.; Harding, R.; Mawer, P. J.; Radford, S. E.; Strong, A. E.; Boden, N. *J. Am. Chem. Soc.* **2003**, *125*, 9619−9628.
(32) Caplan, M. R.; Moore, P. N.; Zhang, S. G.; Kamm, R. D.; Lauffenburger, D. A. *Biomacromolecules* **2000**, *1*, 627−631.
(33) Goeden-Wood, N. L.; Keasling, J. D.; Muller, S. J. *Macromolecules* **2003**, *36*, 2932−2938.
(34) Hartgerink, J. D.; Beniash, E.; Stupp, S. I. *Proc. Natl. Acad. Sci. U.S.A.* **2002**, *99*, 5133−5138.
(35) McMillan, R. A.; Conticello, V. P. *Macromolecules* **2000**, *33*, 4809−4821.
(36) Wang, C.; Stewart, R. J.; Kopecek, J. *Nature (London)* **1999**, *397*, 417−420.
(37) Petka, W. A.; Harden, J. L.; McGrath, K. P.; Wirtz, D.; Tirrell, D. A. *Science* **1998**, *281*, 389−392.
(38) Minor, D. L.; Kim, P. S. *Nature (London)* **1994**, *367*, 660−663.
(39) Bean, J. W.; Kopple, K. D.; Peishoff, C. E. *J. Am. Chem. Soc.* **1992**, *114*, 5328−5334.
(40) Surewicz, W. K.; Stepanik, T. M.; Szabo, A. G.; Mantsch, H. H. *J. Biol. Chem.* **1988**, *263*, 786−790.
(41) Surewicz, W. K.; Mantsch, H. H.; Stahl, G. L.; Epand, R. M. *Proc. Natl. Acad. Sci. U.S.A.* **1987**, *84*, 7028−7030.
(42) Kavanagh, G. M.; Ross-Murphy, S. B. *Prog. Polym. Sci.* **1998**, *23*, 533−562.
(43) Kavanagh, G. M.; Clark, A. H.; Ross-Murphy, S. B. *Langmuir* **2000**, *16*, 9584−9594.
(44) Ross-Murphy, S. B. *Imaging Sci. J.* **1997**, *45*, 205−209.

MA0491762